References

1 Aoki M, Morishita R, Taniyama Y, Kida I, Moriguchi A, Matsumoto K, Nakamura T, Kaneda Y, Higaki J, Ogihara T: Angiogenesis induced by hepatocyte growth factor in non-infarcted myocardium and infarcted myocardium: Up-regulation of essential transcription factor for angiogenesis. Gene Ther 2000;7: 417–427.

2 Hayashi S, Morishita R, Nakamura S, Yamamoto K, Moriguchi A, Nagano T, Taizi M, Noguchi H, Matsumoto K, Nakamura T, Higaki J, Ogihara T: Potential role of hepatocyte growth factor, a novel angiogenic growth factor, in peripheral arterial disease: Down-regulation of HGF in response to hypoxia in vascular cells. Circulation 1999;100:11301–11308.

3 Morishita R, Nakamura S, Hayashi S, Taniyama Y, Moriguchi A, Nagano T, Taiji M, Noguchi H, Takeshita S, Matsumoto K, Nakamura T, Higaki J, Ogihara T: Therapeutic angiogenesis induced by human recombinant hepatocyte growth factor in rabbit hind limb ischemia model as cytokine supplement therapy. Hypertension 1999;33:1379–1384.

4 Hayashi T, Abe K, Sakurai M, Itoyama Y: Inductions of hepatocyte growth factor and its activator in rat brain with permanent middle cerebral artery occlusion. Brain Res 1998;799: 311–316.

5 Miyazawa T, Matsumoto K, Ohmichi H, Katoh H, Yamashima T, Nakamura T: Protection of hippocampal neurons from ischemia-induced delayed neuronal death by hepatocyte growth factor: A novel neurotrophic factor. J Cereb Blood Flow Metab 1998;18:345–348.

6 Yamada T, Yoshiyama Y, Tsuboi Y, Shimomura T: Astroglial expression of hepatocyte growth factor and hepatocyte growth factor activator in human brain tissues. Brain Res 1997; 762:251–255.

7 Jung W, Castrén E, Odenthal M, Vande Woude G, Dienes HP, Lindholm D, Schirmacher P: Expression and functional interaction of hepatocyte growth factor-scatter factor (HGF-SF) and its receptor c-met in mammalian brain. J Cell Biol 1994 126:485–494.

8 Achim CL, Katyal S, Wiley CA, Shiratori M, Wang G, Oshika E, Petersen BE, Li J-M, Michalopoulos GK: Expression of HGF and c-met in the developing and adult brain. Brain Res Dev Brain Res 1997;102:299–303.

9 Honda S, Kagoshima M, Wanaka A, Tohyama M, Matsumoto K, Nakamura T: Localization and functional coupling of HGF and c-met/HGF receptor in rat brain: Implication as neurotrophic factor. Brain Res Mol Brain Res 1995;32:197–210.

10 Jung W, Castren E, Odenthal M, Vande Woude GF, Ishii T, Dienes HP, Lindholm D, Schirmacher P: Expression and functional interaction of hepatocyte growth factor-scatter factor and its receptor c-met in mammalian brain. J Cell Biol 1994;126:485–494.

11 Hamanoue M, Takemoto N, Matsumoto K, Nakamura T, Nakajima K, Kohsaka S: Neurotrophic effect of hepatocyte growth factor on central nervous system neurons in vitro. J Neurosci Res 1996;43:554–564.

12 Korhonen L, Sjoholm U, Takei N, Kern MA, Schirmacher P, Castren E, Lindholm D: Expression of c-Met in developing rat hippocampus: Evidence for HGF as a neurotrophic factor for calbindin D-expressing neurons. Eur J Neurosci 2000;12:3453–3461.

13 Hayashi K, Morishita R, Nakagami H, Yoshimura S, Hara A, Matsumoto K, Nakamura T, Kaneda Y, Ogihara T, Sakai N: Gene therapy for preventing neuronal death using hepatocyte growth factor: In vivo gene transfer of HGF to subarachnoid space prevents delayed neuronal death in gerbil hippocampal CA1 neurons. Gene Ther 2001;8:1167–1173.

14 Powell EM, Campbell DB, Stanwood GD, Davis C, Noebels JL, Levitt P: Genetic disruption of cortical interneuron development causes region- and GABA cell type-specific deficits, epilepsy, and behavioral dysfunction. J Neurosci 2003;23:622–631.

15 Tsuzuki N, Miyazawa T, Matsumoto K, Nakamura T, Shima K: Hepatocyte growth factor reduces the infarct volume after transient focal cerebral ischemia in rats. Neurol Res 2001;23: 417–424.

16 LeDoux JE: The Emotional Brain. New York, Simon and Schuster, 1996.

17 Rosen EM, Nigam SK, Goldberg ID: Scatter factor and the c-met receptor: A paradigm for mesenchymal epithelial interaction. J Cell Biol 1994;127:1783–1787.

18 Zarnegar R: Michalopoulos G: The many faces of hepatocyte growth factor: From hepatopoiesis to hematopoiesis. J Cell Biol 1995;129: 1177–1180.

19 Park M, Dean M, Kaul K, Braun MJ, Gonda MA, Vande Woude GF: Sequence of MET protooncogene cDNA has features characteristic of the tyrosine kinase family of growth-factor receptors. Proc Natl Acad Sci USA 1987;84: 6379–6383.

20 Bowers DC, Fan S, Walter K, Abounader R, Williams JA, Rosen EM, Laterra J: Scatter factor/hepatocyte growth factor activates AKT and protects against cytotoxic death in human glioblastoma via PI3-kinase and AKT-dependent pathways. Cancer Res 2000;60:4277–4283.

21 Fan S, Ma YX, Wang J, Yuan R, Meng Q, Cao Y, Laterra J, Goldberg ID, Rosen EM: The cytokine scatter factor inhibits apoptosis and enhances DNA repair by a common mechanism involving signaling through phosphatidyl inositol 3′ kinase. Oncogene 2000;19:2212–2223.

22 Yamada K, Moriguchi A, Morishita R, Aoki M, Nakamura Y, Mikami H, Oshima T, Ninomiya M, Kaneda Y, Higaki J, Ogihara T: Efficient oligonucleotide delivery using the HVJ-liposome method in the central nervous system. Am J Physiol 1996;271:R1212–R1220.

23 Tsuboi Y, Kakimoto K, Nakajima M, Akatsu H, Yamamoto T, Ogawa K, Ohnishi T, Daikuhara Y, Yamada T: Increased hepatocyte growth factor level in cerebrospinal fluid in Alzheimer's disease. Acta Neurol Scand 2003; 107:81–86.

24 Furge KA, Zhang YW, Vande Woude GF: Met receptor tyrosine kinase: Enhanced signaling through adapter proteins. Oncogene 2000;19: 5582–5589.

J. Phys. Ther. Sci.
17: 109–113, 2005

Expression of Hepatocyte Growth Factor in Rat Skeletal Muscle

SHOJI TANAKA, RPT[1], JUNJI TANAKA, PhD[2], EI KAWAHARA, MD, PhD[2], HIROSHI FUNAKOSHI, MD, PhD[3], TOSHIKAZU NAKAMURA, PhD[3], KATSUHIKO TACHINO, MD, PhD[1]

[1]*Department of Impairment Study, Graduate Course of Rehabilitation Science;*
[2]*Department of Clinical Laboratory Science, Graduate Course of Medical Science and Technology, Division of Health Sciences, Graduate School of Medical Science, Kanazawa University: 5-11-80 Kodatsuno, Kanazawa City, Ishikawa 920-0942, Japan.*
TEL +81 76-265-2500 E-mail: tanakas@mhs.mp.kanazawa-u.ac.jp
[3]*Division of Molecular Regenerative Medicine, Course of Advanced Medicine, Osaka University Graduate School of Medicine*

Abstract. The present study examined the localization of hepatocyte growth factor in rat skeletal muscle, and investigated whether levels of hepatocyte growth factor differ between skeletal muscles. Levels of hepatocyte growth factor in soleus and tibialis anterior muscles were measured using enzyme-linked immunosorbent assay. Localization of hepatocyte growth factor and proliferating cell nuclear antigen in the soleus muscle was visualized using immunofluorescence analysis. Level of hepatocyte growth factor was 3.2 ± 1.4 ng/g tissue in the soleus muscle and 3.4 ± 0.4 ng/g tissue in the tibialis anterior muscle. No significant differences were identified between muscles with differential contractile characteristics. Existence of hepatocyte growth factor was observed in cytoplasm of small cells conterminous to muscle fibers. Cells in a similar position displayed reactivity to proliferating cell nuclear antigen, suggesting that they represented activated skeletal muscle satellite cells. Hepatocyte growth factor is produced in normal rat skeletal muscle by activated skeletal muscle satellite cells.
Key words: Skeletal muscle, HGF, PCNA

(This article was submitted Jul. 5, 2005, and was accepted Sep. 29, 2005)

INTRODUCTION

Skeletal muscle cells play important roles in muscle regeneration and hyperplasia[1]. Skeletal muscle satellite cells are usually present in a quiescent state between the plasma membrane and basal lamina[2], but become activated following muscular injury or mechanical stretch[3–5]. Activated satellite cells enter into a cycle of proliferation and division, and differentiate into myoblasts[6, 7]. These myoblasts undergo coalescence and maturation, finishing with repair and hyperplasia. Growth factors such as hepatocyte growth factor (HGF)[5], fibroblast growth factor[8, 9] and insulin-like growth factor I[10] are associated with the proliferation and differentiation of satellite cells. However, each factor plays a different role. While HGF can cause precocious entry into the cell cycle for satellite cells, the actions of HGF in skeletal muscle *in vivo* remain unclear. Although the contractile function of skeletal muscles differs between specific muscles, relationships between the contractile properties of skeletal muscle and concentrations of HGF are unknown. Clarification of these mechanisms could prove very useful in determining physical therapy to achieve hypertrophy or hyperplasia. Furthermore,

repair reactions of specific skeletal muscles may differ with function. The present study investigated associations between production of HGF and contractile properties in rat skeletal muscle.

METHODS

Animals and materials

The present study used 6 female, 11-week-old Wistar rats (body weight, 196–220 g). Deep anesthesia was induced in all animals by intraperitoneal injection of pentobarbital sodium (5 mg/100 g body weight). For quantitative analysis of HGF levels in tissue, 5 of the rats were exsanguinated. The right soleus and tibialis anterior (TA) muscles were then excised and quick-frozen in liquid nitrogen. For immunofluorescence analysis, right soleus muscle was excised from the other normal rat and oriented for cross-section in embedding medium (Tissue Tek OCT compound; Miles, Elkhart, IN, USA), then quick-frozen in isopentane chilled with liquid nitrogen. Samples were stored at –70°C until use. At the end of the study, all animals were sacrificed. All procedures for animal care and treatment were performed in accordance with the Guidelines for the Care and Use of Laboratory Animals at Kanazawa University.

Enzyme-linked immunosorbent assay for hepatocyte growth factor

For detection of HGF levels, tissues were completely homogenized in lysis buffer (pH 7.5). Samples containing HGF were separated by centrifugation for 60 min at 16,100 × g and 4°C. Measurement of HGF levels was performed using an enzyme-linked immunosorbent assay (ELISA) kit (Institute of Immunology, Tokyo, Japan).

Histological analysis

Sections (10 μm thick) were cut on a cryostat, then dried for 1 h at room temperature. For morphological observation, cross sections were stained using hematoxylin and eosin.

Immunofluorescence staining for hepatocyte growth factor and proliferating cell nuclear antigen

Sections (6 μm thick) were cut using a cryostat, and dried for 1 h at room temperature. For detection of HGF, sections were fixed in methanol for 5 min at 4°C. For detection of HGF and proliferating cell nuclear antigen (PCNA; Dako Cytomation Japan, Kyoto, Japan), sections were treated with phosphate-buffered saline (PBS) containing 0.1% TritonX-100 (pH 7.4) for 5 min at room temperature. Non-specific binding sites were blocked using normal swine serum and bovine serum albumin (BSA) in PBS for 10 min. Sections were incubated with each primary antibody, polyclonal anti-rat HGF antibody (Institute of Immunology) diluted 1:10 in PBS and monoclonal anti-mouse PCNA antibody (Dako Cytomation Japan), each for 90 min at 37°C then 30 min at room temperature. Sections were covered with secondary antibody for 20 min at 37°C, using goat anti-rabbit Alexa Fluor 488 (Molecular Probes, Eugene, OR, USA) diluted 1:300 in PBS and goat anti-mouse Alexa Fluor 546 (Molecular Probes) diluted 1:500 in PBS. All nuclei were counterstained using 4',6-diamidino-2-phenylindole dihydrochloride (DAPI; Molecular Probes). Negative controls were incubated with each rabbit serum and mouse IgG. Fluorescein signals in sections were observed and photographed using a fluorescence microscope (Olympus, Tokyo, Japan).

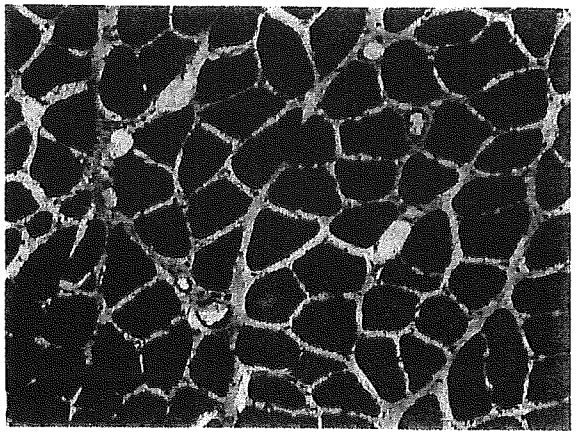

Fig. 1. Soleus muscle. Hematoxylin and eosin, × 200. Scale bar: 50 μm.

Statistical analysis

Student's t-test was used for comparisons between HGF levels in soleus and TA muscles. Values of $P<0.05$ were considered statistically significant.

RESULTS

Tissue HGF level was 3.2 ± 1.4 ng/g of tissue in the soleus muscle and 3.4 ± 0.4 ng/g of tissue in the

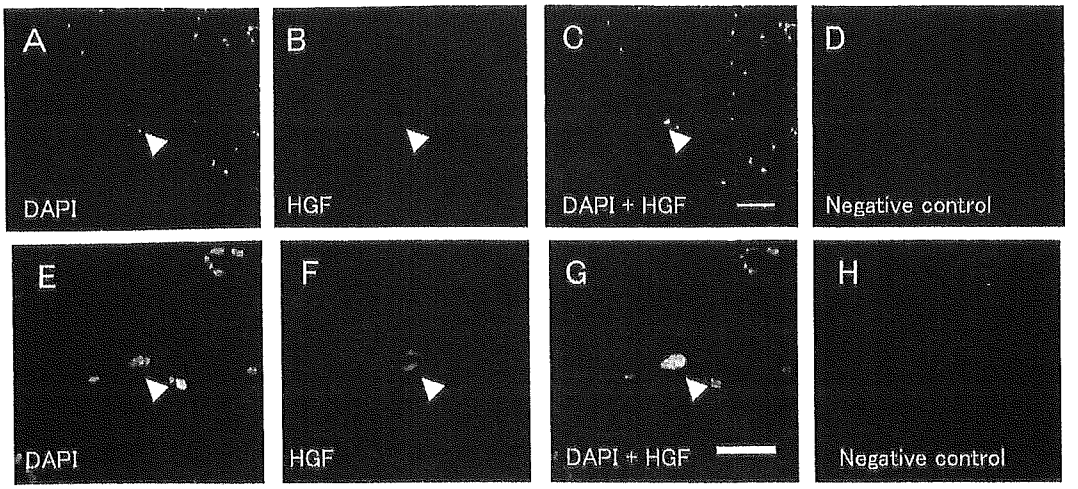

Fig. 2. Immunofluorescence staining for HGF and nuclei in soleus muscle. Many nuclei were observed in general sections (A, C, E, G). HGF was observed in cytoplasm of small cells conterminous to muscle fibers (F). Background in the negative control section was much lower (D, H). Scale bar: A–D, 50 μm; E–H, 10 μm. Magnification × 200.

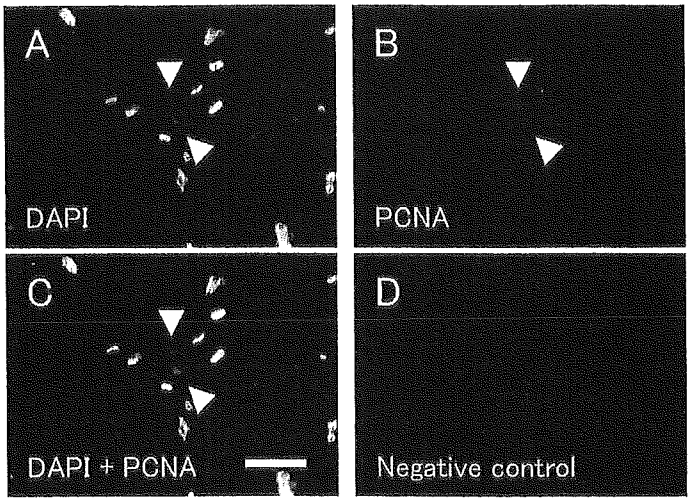

Fig. 3. Immunofluorescence staining for PCNA and nuclei in soleus muscle. Many nuclei are apparent in general sections, but few PCNA-labeled cells are present (A–C). PCNA-labeled cells are present conterminous to muscle fibers (B, C). Background in the negative control section was much lower (D). Scale bar: 20 μm. Magnification × 200.

TA muscle, with no significant differences noted between muscles.

HGF-positive cells were identified as small cells conterminous to muscle fibers (Fig. 2C, G), and HGF signals were localized to the cytoplasm of these small cells (Fig. 2B, C, F, G). Nuclei displayed no positive staining for HGF. Negative control sections displayed lower background levels of normal rabbit serum (Fig. 2D, H). Some cells in a similar position to HGF-positive cells displayed positive reactivity for PCNA (Fig. 3B, C).

DISCUSSION

C-Met is an HGF receptor, which is expressed in normal adult rat TA muscle satellite cells, and HGF is released from satellite cells by mechanical stretch *in vivo*[5, 11]. Expression of slow myosin heavy chains represents 78% of total myosin heavy chain isoforms expressed in the rat soleus, compared to 5% in TA[12]. The number of satellite cells proliferating in the soleus muscle is elevated after functional loading[13]. Thus, in the soleus muscles, which act as "antigravity" postural muscles, HGF concentrations might be assumed to be higher than in TA muscles. However, no significant differences were identified for HGF levels in soleus and TA muscles in the present study. This result suggests that HGF levels in soleus and TA muscles under stationary conditions are around 3.2–3.4 ng/g tissue, with no real difference between muscles displaying differing contractile characteristics.

HGF acted as an activator of quiescent satellite cells *in vivo*[14]. Cells labeled with PCNA, which can be used to detect entry into the cell cycle, were usable as markers for satellite cell activation[15]. We therefore assumed that HGF and PCNA were present in activated satellite cells. In the present study, HGF- and PCNA-positive cells were observed in the same region of the soleus muscle. This indicates that HGF is expressed and activated satellite cells are present in normal rat soleus muscles.

Soleus muscle activity can increase to about 3-fold higher than TA muscle activity during exercise[16]. Muscles of the rat hindlimb were injured by downhill exercise on a treadmill, and the percentage of morphologically altered fibers was 4–8% in soleus muscles, and 1–2% in TA muscles[12, 13]. The number of proliferating satellite cells was then seen to increase within 2 days of injury[12]. Running exercise might thus account for up-regulation of HGF in the soleus muscle.

The present results reveal that HGF levels in normal rat soleus and TA muscles are 3.2–3.4 ng/g of tissue, with no significant differences between muscles. Furthermore, HGF appears to be present in the normal rat soleus muscle, produced by muscle satellite cells. Further research is required to clarify the mechanisms of hypertrophy, hyperplasia and muscle remodeling.

ACKNOWLEDGMENTS

We would like to thank Mr. Masashi Miyazaki from the Department of Physical Therapy at Kagoshima University Hospital, for his assistance in the present study.

REFERENCES

1) Allen RE, Rankin LL: Regulation of satellite cells during skeletal muscle growth and development. Proc Soc Exp Biol Med, 1990, 194: 81–86.
2) Schultz E, Gibson MC, Champion T: Satellite cell are mitotically quiescent in mature mouse muscle: an EM and radioautographic study. J Exp Zool, 1978, 206: 451–456.
3) Anderson JE: A role for nitric oxide in muscle repair: nitric oxide-mediated activation of muscle satellite cells. Mol Biol Cell, 2000, 11: 1859–1874.
4) Sheehan SM, Tatsumi R, Temm-Grove CJ, et al.: HGF is an autocrine growth factor for skeletal muscle satellite cells *in vivo*. Muscle Nerve, 2000, 23: 239–245.
5) Tatsumi R, Anderson JE, Nevoret CJ, et al.: HGF/SF is present in normal adult skeletal muscle and is capable of activating satellite cells. Dev Biol, 1998, 194: 114–128.
6) Bischoff R: Proliferation of muscle satellite cells on intact myofibers in culture. Dev Biol, 1986, 115: 129–139.
7) Bladt F, Riethmacher D, Isenmann S, et al.: Essential role for the c-met receptor in the migration of myogenic precursor cells into the limb bud. Nature, 1995, 376: 768–771.
8) Yablonka-Reuveni Z, Seger R, Rivera AJ: Fibroblast growth factor promotes recruitment of skeletal muscle satellite cells in young and old rats. J Histochem Cytochem, 1999, 47: 23–42.
9) Kastner S, Elias MC, Rivera AJ, et al.: Gene expression patterns of the fibroblast growth factors and their receptors during myogenesis of rat satellite cells J Histochem Cytochem, 2000, 48: 1079–1096.
10) Chakravarthy MV, Davis BS, Booth FW: IGF-restores satellite cell proliferative potential in immobilized old skeletal muscle. J Appl Physiol, 2000 89:1365–1379.
11) Tatsumi R, Sheehan SM, Iwasaki H, et al.: Mechanical stretch induces activation of skeletal muscle satellit cells *in vitro*. Exp Cell Res, 2001, 267: 107–114.
12) Smith HK, Maxwell L, Rodgers CD, et al.: Exercise enhanced satellite cell proliferation and new myonuclear accretion in rat skeletal muscle. J Appl Physiol, 2001, 90: 1407–1414.
13) Smith HK, Plyley MJ, Rodgers CD, et al.: Skeletal muscle damage in the hindlimb following single or repeated daily bouts of downhill exercise. Int J Sport Med, 1997, 18: 94–100.

14) Allen RE, Sheehan SM, Taylor RG, et al.: Hepatocyte growth factor activates quiescent skeletal muscle satellite cells *in vitro*. J Cell Physiol, 1995, 165: 307–312.
15) Johnson SE, Allen RE: Proliferating cell nuclear antigen (PCNA) is expressed in activated rat skeletal muscle satellite cells. J Cell Physiol, 1993, 154: 39–43.
16) Canu MH, Falempin M: Effect of hindlimb unloading on two hindlimb muscles during treadmill locomotion in rats. Eur J Appl Physiol Occup Physiol, 1997, 75: 283–288.

日本臨牀　63巻 増刊号8（2005年8月28日発行）別刷

広範囲 血液・尿化学検査 免疫学的検査

—その数値をどう読むか—
[第6版]

(4)

IX. プロスタノイド，サイトカイン，増殖因子，ケモカイン

肝細胞増殖因子(HGF)

大谷若菜　　船越　洋　　中村敏一

肝細胞増殖因子(HGF)

Hepatocyte growth factor(HGF)

大谷若菜　船越　洋
中村敏一

Key words: 肝細胞増殖因子，c-Met，劇症肝炎，血清

1. 概　　説

肝細胞増殖因子(hepatocyte growth factor: HGF)は1984年当研究室の中村らにより肝細胞増殖活性を指標にラットの血小板より精製され[1]，1989年にラットならびにヒトHGFがクローニングされた[2]．その構造は，クリングルドメインを4つ含むα鎖(69kDa)と，セリンプロテアーゼ様構造をもつβ鎖(34kDa)からなる．細胞からは一本鎖のプロ体として分泌され，HGF converting enzymeもしくはHGF activator，u-PA(urokinase-type plasminogen activator)，t-PA(tissue-type PA)，matriptaseなどによりα鎖とβ鎖間のArg-Val部位で切断され二本鎖HGFとなり初めてc-Met/HGF受容体との結合活性をもつ(図1-a)．

HGFの生物活性は当初の肝細胞増殖活性のみでなく，肝細胞以外にも多数の上皮細胞，内皮細胞，一部の間葉細胞に増殖活性作用を，更には細胞分化，細胞遊走，器官形成，抗アポトーシス，血管新生作用をももつことが明らかとなってきている[4]．このように多彩な作用を兼ね備えたHGFは組織傷害に対して生体の再生機構の主役を果たすと考えられている．

これまでにHGFは，肝臓をはじめ，腎臓，肺，心臓，脳といった様々な臓器疾患，特に治療法がなかった難治性疾患に対してもダイナミックな治療効果をあらわし，一方でHGFアンタゴニストとして機能するNK4(HGFα鎖)は，癌の浸潤，転移，血管新生の阻害による抗癌作用をあらわすことが動物レベルで多数報告されている．上記疾患に反応して生体はHGFを放出し傷害を治癒しようとすることで血中HGFは変動するが，その際内在性HGF量が不十分な場合は補充療法による治療が有効となるだろう．本稿では，これら様々な疾患によるHGFの血中変動を中心に解説し，診断・治療を行う際の一助となることを目的としている．

2. 試料の採取方法，保存条件

採血は溶血を避け，速やかに血清分離を行う．検体の保存には，ポリプレン製かポリエチレン製チューブまたはシリコンコートしたガラス製チューブを使用し，4℃で1週間，1週間以上の際は，−20℃以下で保存する．検体の凍結融解の繰り返しは避ける．

3. 測定法—ELISA法によるHGF蛋白質量の定量法

著者らの研究室で行っているhuman HGF ELISA法は，固相(ELISA plate)に固定化した抗HGF 1次抗体に抗原であるHGFを捕捉させ，更にビオチン化抗HGF 2次抗体と結合後，酵素反応を経て試料中の抗原分子濃度を定量する方法である．この方法により簡便な操作で高感度(HGF検出濃度；0.1ng/ml)かつ再現性の高い結果が得られる[5](ヒト，ラットHGF ELISA kit: 株式会社特殊免疫研究所；Tel: 03-3814-4081)．また，活性型HGFのみを検出するELISA法が大西らにより報告されている[6]．

4. HGFの血中動態

^{125}I-HGF静脈注射3分後の組織分布で，HGFは肝臓，副腎，脾臓，腎臓，肺，胃，小腸に分

Wakana Ohya, Hiroshi Funakoshi, Toshikazu Nakamura: Division of Molecular Regenerative Medicine, Course of Advanced Medicine, Osaka University Graduate School of Medicine　大阪大学大学院医学系研究科 未来医療開発専攻組織再生医学講座 分子組織再生分野

0047-1852/05/¥40/頁/JCLS

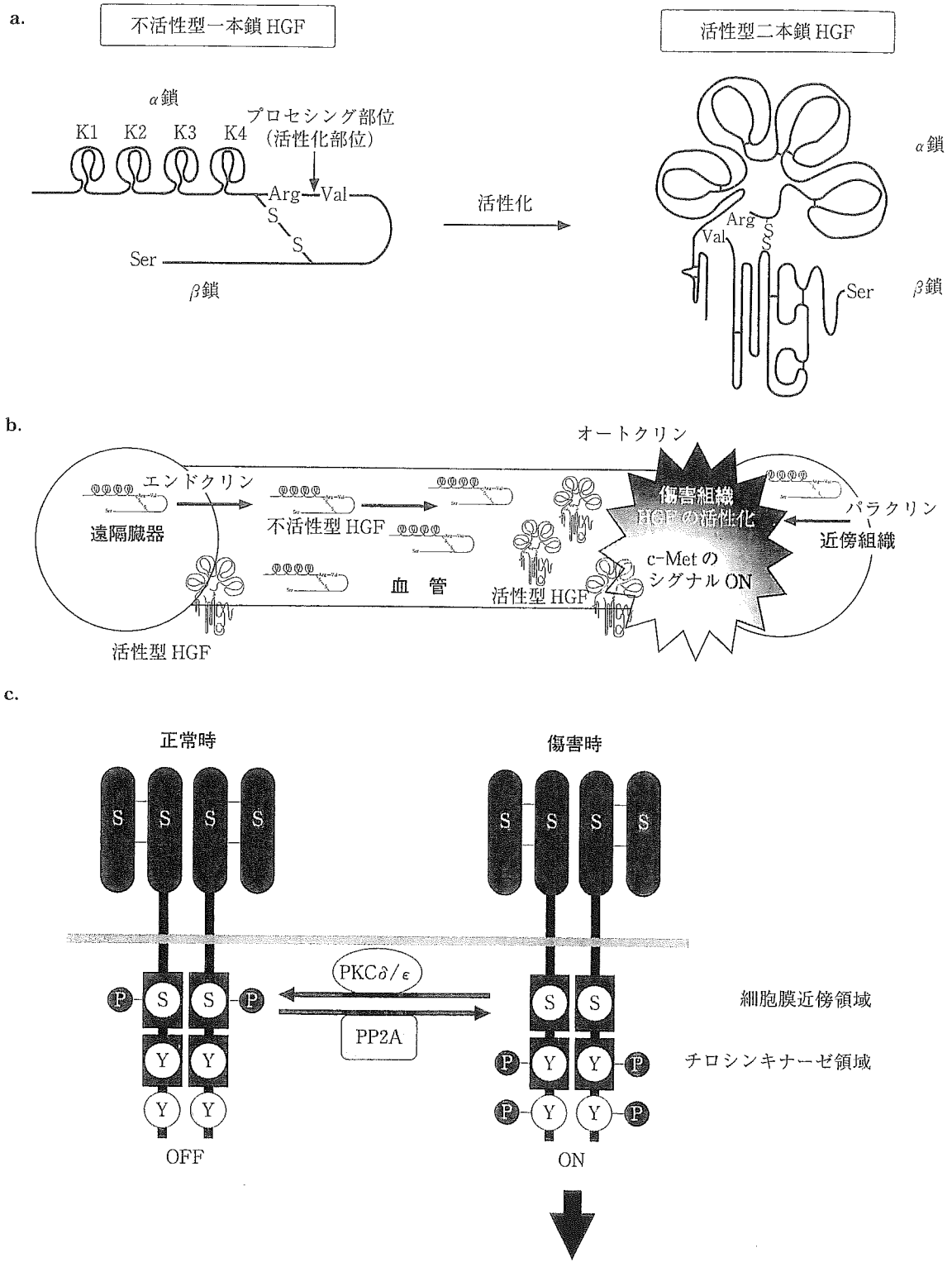

図 1　HGF の構造と傷害組織特異的作用分子機構の模式図

a: HGF の構造と活性化機構．b: 傷害臓器への活性化 HGF の供給．弱い傷害では HGF はパラクリンやオートクリンによって局所的に供給されるが，強い傷害や慢性傷害では，遠隔の臓器によるエンドクリンによる供給も行われる．主に傷害組織で不活性型 HGF は活性型 HGF へ変換される．c: 傷害認知機構としての c-Met のシグナルスイッチ．正常組織では c-Met 細胞膜近傍領域のセリンがリン酸化されていることで HGF による c-Met のチロシンのリン酸化が阻害されている（シグナル OFF）．一方で，傷害組織ではこのセリンが PP2A によって脱リン酸化されているため HGF により c-Met のチロシンのリン酸化が起こりシグナルが伝達される（シグナル ON＝c-Met 活性化）．つまり傷害特異的な c-Met のセリンリン酸化により HGF は傷害組織特異的に c-Met を活性化する．

布する．一方，心臓や脳への分布は大部分が細胞外スペースへの見かけの分布である．部分肝切除，肝硬変ラットにおいては，ヒトHGF静脈注射後少なくとも2時間は正常ラットの10倍の血清ヒトHGF量が維持される[7]．

血液中のHGFのクリアランスの約70％は肝臓(他，腎臓で10％以下)で行われる．ここでは，c-Metを介した内在化機構(エンドサイトーシス)とともに，ヘパラン硫酸との結合による低親和性クリアランスの両者が想定されている．肝傷害時やリコンビナントHGF大量投与時のように血液中HGFが高濃度に存在すると，肝臓におけるc-Metの発現が低下し内在化機能低下によるクリアランスが低下する．劇症肝炎発症時の血清HGF値の著明な増加は，HGF産生の増加に加え，c-Metの発現低下，肝細胞数の減少によるクリアランスの低下も大きく関与すると考えられる[4]．

5. HGFの生理的変動

正常血清レベルは，年齢による変化は少ないが20歳代でピークになり以後徐々に減少し，男女間で有意差はない．ただし女性の場合，子宮内膜の増殖，再生，修復を反映し，月経時に高く排卵時に低いという性周期に伴った変化をする．また妊娠時には，母体血液中HGF濃度は妊娠経過とともに上昇し，妊娠後期でピークを示すのに対して，羊水中では妊娠中期にピークを示し(胎盤でのHGF発現も同様)このとき母体の100倍となり胎児肺，腸管形態形成に強く関与することが推察される[4](**表1**)．また肥満のように，HGFを産生する細胞(脂肪細胞)の過増殖による場合も増加する．

6. HGFのその他の因子による変動

IL-1β，グルココルチコイドなど様々な因子，薬物がHGF産生を誘導，あるいは抑制することが報告されており[9]，これらの投与によるHGF値変動も忘れてはならない．

表1 HGF検査値の生理的変動

	HGF(ng/ml)		
年 齢	女性血清中		男性血清中
10代	0.36±0.16		0.35±0.25
20代	0.39±0.25		0.37±0.22
30代	0.37±0.19		0.33±0.19
40代	0.33±0.17		0.29±0.17
50代	0.26±0.17		0.29±0.15
妊娠時期	血清中	羊水中	臍帯血中
妊娠初期	0.30以下	15±8	0.30以下
妊娠中期	0.41±0.21	48±23	
妊娠後期	0.48±0.25	6±3	

7. HGFの正常および各種疾患における検査値と臨床的意義(表2[4])

a. 傷害時血清HGF値の変動

器官再生促進作用をもつHGFの血中濃度は様々な臓器の傷害時に敏感に反応変動する．器官に傷害が発生したとき，傷害臓器のみならず遠隔の正常臓器でも傷害が認知され即座にHGFが産生，放出され，このHGFはエンドクリン，パラクリンを駆使して傷害組織に供給される(**図1-b**)．血中に豊富に供給されたHGFのシグナルが傷害臓器でのみ強く受け取られるという巧妙な仕組みは，HGFの活性化とc-Metの傷害認知機構としてのシグナルスイッチ[8]，c-Metの発現誘導によって支えられている(**図1-b，c**)．また，傷害に依存したc-Metの特異的シグナルスイッチは活性型リコンビナントHGF蛋白が傷害組織で効率よく機能することに有利に働いている．

b. 各種疾患による変動

1) 肝 疾 患

急性肝炎，慢性肝炎，肝硬変，肝細胞癌などでは肝傷害の重症度に相関してHGF値のレベルが増加する．このことは急性肝炎ではビリルビン，AST，γ-GTP，慢性肝炎では組織活性インデックスといった肝機能検査との相関によって明らかである．一方で，劇症肝炎では，肝細胞の著減によるc-Met依存的なHGFのクリアランスの極度低下という因子も加わり血清HGF値

表2 正常および各種疾患における血清，組織などのHGF値

	疾患名	検査値(ng/ml; ng/mg)	
	正常	0.27±0.08*	
各種疾患の患者血清	アルコール中毒	0.78	
	肥満	2.46±0.18(0.77正常)	Rehman Jら(2003)
	急性肝炎	0.45±0.23*	
	慢性肝炎	0.40±0.16*	
	肝硬変	1.05±0.64*	
	肝細胞癌	1.06±1.45*	
	原発性胆汁性肝硬変	0.44±0.22*	
	劇症肝炎	16.40±14.67*	
	肝臓移植後順調な回復時	0.33±0.04	
	肝臓移植後プロトロンビン時間の異常上昇時	2.01±0.99	
	胆管閉塞	0.32±0.13(0.17±0.03)	Kimura Fら(2000)
	間質性肺炎	1.16±0.22(p<0.01)	
	細菌性肺炎	0.96±0.27(p<0.01)	
	肺線維症	0.34±0.002(p<0.01)	
	急性腎不全(急相期)	0.55±0.24	
	慢性尿細管間質性腎炎	0.44±0.37	
	慢性腎不全(非透析時)	0.33±0.1	
	慢性腎不全(透析1年未満)	0.33±0.13	
	慢性腎不全(透析5年から10年)	0.45±0.13	
	移植後急性腎拒絶	2.17±1.14	
	腎異系移植片機能良好時ピーク	2.48-5.63	
	高血圧(WHO stage I)	0.48±0.03(p<0.01)	
	高血圧(WHO stage II, III)	0.88±0.1(p<0.01)	
	動脈硬化症	0.35±0.11	
	狭心症	0.3±0.1	
	急性心筋梗塞(6時間以内)	10.4±8.8	
	急性心筋梗塞(6-12時間)	6.7±4.5	
	軽，中等度急性膵炎	0.63±0.06	
	重度急性膵炎	2.30±0.61	
	インスリン治療前値	0.74±0.14	
	I型糖尿病罹患短期(発症半年から3年)	0.78±0.40	
	I型糖尿病罹患長期(腎障害を伴わない)	0.86±0.42	
	I型糖尿病罹患長期(腎障害を伴う)	0.79±0.27	
	多発性筋炎	0.63±0.11	
	皮膚筋炎	0.58±0.07	
	不活性型全身性エリテマトーデス	0.79	
	活性型全身性エリテマトーデス	1.02	
	潰瘍性大腸炎	1.38±0.11	
	Crohn病	1.44±0.08	
	HELLP症候群	1.79±0.35	
	アミロイドーシス	2.26±2.73(0.18±0.07)	Shikano Mら(2000)
	生存1年以上，1年未満	0.46±0.26，2.83±2.85	
気管支肺胞洗浄液	正常	0.23±0.09	
	特発性肺線維症	0.77±0.88(p<0.001)	
	リウマチ性関節炎	0.50±0.64(p<0.001)	
	サルコイドーシス	0.41±0.61(p<0.05)	
大脳皮質	正常(平均72.0歳)	9.60±4.62	
	Alzheimer病(平均78.7歳)	33.7±18.47	
	進行性Parkinson病(平均78.5歳)	20.23±13.55	
	Huntington病(平均73.8歳)	36.15±11.98	

( )：正常対照群，*：RIA(radioimmunoassay)による値，
*以外：ELISAによる値，**：活性化型HGF量．(文献[3,10])

(次ページにつづく)

（表2つづき）

	疾患名	検査値（ng/ml; ng/mg）	
脳脊髄液	正常	0.35±0.126（0.034±0.012**）	
	非感染性髄膜炎	0.42±0.07	
	細菌性髄膜炎	6.10±5.20	
	筋萎縮性側索硬化症	0.58	
	Alzheimer病	0.06±0.017**	Tsuboi Yら（2003）
	もやもや病	0.87±0.32	Namba Rら（2004）
尿	正常**	19.3±7.1（pg/mg creatinine**）	
	急性尿細管壊死（正常尿量時）	6.9±0.7（ng/g creatinine）	
	急性尿細管壊死（乏尿時）	19.1±4.2（ng/g creatinine）	
胆汁	正常	0.8±0.1	
	肝切除後1日目（非糖尿病）	4.0±0.4（$p<0.05$）	
溝歯液肉	正常	7.37±1.46（1.70±0.73**）	Oshima Mら（2004）
	歯周病	117.3±16.9（3.23±1.01**）	Kakimoto Kら（2004）
涙	正常	0.19-0.29	LI Qら（1996）
	手術1日後（白内障，角膜手術）	0.45-0.62	
硝子体	正常	2.16±1.39	
	裂孔原性網膜剥離	2.02±0.84	
	増殖性硝子体網膜症	3.94±2.29	
	非糖尿病例	1.6	
	糖尿病性増殖性網膜症（ルベオーシス－）	4.2（$p<0.05$）	
	糖尿病性増殖性網膜症（ルベオーシス＋）	7.2（$p<0.01$）	
関節液	変形性関節症	0.19	
	細菌性関節炎	0.18	
	リウマチ性関節炎	1.21	
胎盤	正常	6.16±3.32（ng/mg）	
	妊娠中毒症	4.05±1.44（ng/mg）（$p<0.05$）	
癌患者の血清	食道癌（stage I/II）	0.47±0.13	
	食道癌（stage III/IV）	0.88±1.05	
	食道癌（再発性）	1.51±1.62	
	胃癌（stage I/II）	0.32±0.15	
	胃癌（stage III/IV）	0.49±0.46	
	胃癌（再発性）	0.44±0.29	
	肝細胞癌	1.06±1.45	
	肝芽腫（治療前）	0.89	
	肝芽腫（化学療法後）	0.46	
	結腸直腸癌（stage I/II）	0.35±0.15	
	結腸直腸癌（stage III/IV）	0.38±0.19	
	結腸直腸癌（stage V）	0.50±0.25	
	結腸直腸癌（再発性）	0.44±0.14	
	乳癌（原発性）	0.38±0.31	
	乳癌（再発性）	0.59±0.42	
	前立腺癌（転移なし）	0.97	
	前立腺癌（転移あり）	2.12	
	小細胞肺癌（平均）	0.40±0.17	
	小細胞肺癌（限局性）	0.34±0.12	
	小細胞肺癌（広範囲）	0.47±0.20	
	急性骨髄芽球性白血病	2.03（1.055）	
	多発性骨髄腫（stage I）	1.43	Alexandrakis MGら（2003）
	多発性骨髄腫（stage II）	1.74	
	多発性骨髄腫（stage III）	1.99	
	Hodgkin病	1.40±0.09（0.67±0.03）	Teofili Lら（2001）
	Hodgkin病回復時	0.62±0.03	
	Hodgkin病再発時	1.50±0.24	
	リンパ腫（Hodgkin病以外）	1.02（0.69）	Hsiao LTら（2003）
腫瘍	正常乳房	0.11	
	乳癌	0.35	

が正常時の60倍となる．またこのときのHGFはほとんどが不活性型である[4]．予後因子としてのHGFは，予後が極めて良くない肝炎の劇症化(脳症の発現)を血清HGFが1ng/mlを超えた時点で診断し，早期に治療を開始する指標として重要であるとされている．

2) 腎疾患

腎不全では，血清HGF値は正常の2-3倍程度に上昇する．このうち急性腎不全ではほとんどが活性型になっているのに対して，慢性腎不全ではほとんどが不活性型であり，腎臓よりむしろ肝臓，脾臓でHGF濃度が上昇しておりエンドクリン的供給が行われている．透析の際，静脈内注射，体外循環液中にヘパリンを用いた場合，HGFとの親和性の差により組織中のヘパラン硫酸と低親和性に結合しているHGFが流出するため，血中HGF値が上昇する．また移植腎の急性拒絶反応でも，免疫反応による腎障害によってHGFが産生され血中HGF値は上昇するが，腎毒性をもつ免疫抑制剤やHGF産生を抑制するデキサメタゾンを使用した際はHGF値が修飾されるため，その点に留意した診断が必要である[4]．

3) 肺疾患

血清HGF値が間質性肺炎と細菌性肺炎で高値を示す．肺炎治療に応答した患者では血清HGF値は低下，改善するが，死亡患者では不変であり，血清HGF値と肺炎の予後に相関を認める[4]．

4) 膵疾患

膵炎の重症度評価に血清HGF値は血清CRP値と同程度，IL-6値より有用と報告されている[4]．

5) 血管性疾患

血管障害でのHGFの供給は特にエンドクリンの要素が強いため，血中HGF値にあらわれやすい．HGFは血管内皮細胞増殖作用をもつことから，高血圧においても，血清HGF値は上昇しており，収縮期，拡張期血圧のいずれとも相関を示し重症度を反映している．また糖尿病では，グルコース毒性により内皮細胞が傷害され合併症として高血圧，動脈硬化につながることが多いが，この際HGF値は糖尿病でわずかに減少するも高血圧を合併した場合は上昇し，糖尿病における合併症進展への診断につながる．更に糖尿病性閉塞性動脈硬化症(ASO)，増殖性網膜症でも血中HGF値は高値を示すが，閉塞血管では減少していることから，HGFの補充療法は治療効果を示す[4]．ヒトASOに対するHGF遺伝子治療も大阪大学病院で開始され，高い治療効果が証明されている．

6) 神経疾患

脳は，血液の供給において脳血液関門が存在するため他臓器と切り離された環境にある．したがって脳疾患は血清HGF値に反映されにくい．脳内の傷害を反映すると考えられる脳脊髄液では，HGF値は髄膜炎のうち非感染性では変化しないのに対して細菌性で著増する．筋萎縮性側索硬化症(ALS)，もやもや病で2倍程度に増加する．更にAlzheimer病では活性型HGFが2倍に増加する．このとき．HGFアクチベーター阻害因子(HGF activator inhibitor)の脳内発現が低下することが報告されている[4]．HGFは多くの難治性神経疾患の標的神経細胞に対する強力な神経栄養因子でありALSなどの治療に大きな期待が寄せられている．またHGFが抗不安作用をもつことが明らかとなり，今後は精神神経疾患におけるHGF値の測定も重要となると考えられる．

7) 心疾患

血清HGF値は狭心症では増加しないのに対し，急性心筋梗塞においては血清CKおよびCK-MB値と経時的に相関して高値を示す．特にHGF値の増加は他の2者より早く，狭心痛発作後3時間以内の増加率が高い．このため血清HGF値は心筋梗塞の早期マーカーとしても有効と考えられる．著者らの研究室では*in vivo*で心筋細胞死阻止および血管新生促進作用の両作用を確認しており，これら二重効果を利用したHGFの心筋梗塞への臨床応用が期待できる[4]．

8) 癌

正常組織において主に線維芽細胞，内皮細胞，マクロファージなどの間質細胞により産生されるHGFは，癌組織においては，癌細胞自身が産生し自身で受け取るというオートクリンループを形成する場合もみられる．血中HGF値は様々な細胞種の癌で増加が認められる．**表2**で示したいずれの癌においても，悪性化(ステージの進

行)に伴って血中HGF値は上昇し，回復時にはHGF値が減少する．また再発例，転移例においては更に高い値を示し，特に乳癌において転移が肝臓に起こった場合は，血中HGFの上昇が顕著にみられる．大腸癌，乳癌などでは血中HGF値に病理像との関連も認められ癌の重症度をよく反映しているといえる[4]．

9) その他の疾患

HGF値の報告は，ここ数年でこれまで研究が盛んであった主要臓器以外の疾患や，我々万人に身近な生活習慣病においても相次いでなされている．更に血液以外の滲出液の変化を知ることは傷害を把握するうえでより直接的であると考えられる．アミロイドーシスで血清HGF値は高値となり，特に1年生存率との間には負の相関がみられる．肥満では，脂肪細胞がHGFを産生することにより，血清HGF値とBMI(体格指数)の間に正の相関がみられている．また歯周病では歯肉溝液で，リウマチ性関節炎患者では関節液で，HGF値は高値を示す．

おわりに

これまでの様々な疾患モデル動物を用いた実験でのHGFによる治療効果の報告には目を見張るばかりである．傷害応答因子としてのHGFの血中動向を把握することは，傷害発生そのものを把握することに近い．HGFは様々な臓器障害に対して放出されるため傷害部位の特定には注意を要するが，他の検査を組み合わすことで傷害診断，疾病予後の予知に有効であると考えられる．

傷害時における血中HGFが活性化されているか否かの情報は，ある種の疾患にとっては有用であるが，c-Met側の傷害認知機構が明らかとなった今日ではHGF側の情報だけでは不十分であり検査感度的にも難しいことから，血中の総HGF量の値を知ることはこれまでと同様重要であろう．血中HGF値が変動する疾患の多くで，HGF，NK4の投与によりその症状が改善されることが動物レベルで明らかである．血中HGFの値を知ることで様々な疾病の早期診断の一助とし，HGF，NK4を治療薬として利用できる日ができるだけ早くくることを切に望む．

文献

1) Nakamura T, et al: Biochem Biophys Res Commun **122**: 1450-1459, 1984.
2) Nakamura T, et al: Nature **342**: 440-443, 1989.
3) 中村敏一，荻原俊男(監): HGFの分子医学，メディカルレビュー社，1998.
4) Funakoshi H, Nakamura T: Clin Chim Acta **327**: 1-23, 2003.
5) Yamada A, et al: Biomed Res **16**: 105-114, 1995.
6) Onishi T, et al: J Immunol Methods **244**: 163-173, 2000.
7) Ido A, et al: Hepatol Res **30**: 175-181, 2004.
8) Hashigasako A, et al: J Biol Chem **279**: 26445-26452, 2004.
9) Matsumoto K, et al: Proc Natl Acad Sci USA **89**: 3800-3804, 1992.
10) 船越　洋，中村敏一：日本臨牀 **57**: 821-826, 1999.

Acta Neuropathol (2005) 110: 101–112
DOI 10.1007/s00401-005-1019-3

REGULAR PAPER

Shinsuke Kato · Masako Kato · Yasuko Abe
Tomohiro Matsumura · Takeshi Nishino · Masashi Aoki
Yasuto Itoyama · Kohtaro Asayama · Akira Awaya
Asao Hirano · Eisaku Ohama

Redox system expression in the motor neurons in amyotrophic lateral sclerosis (ALS): immunohistochemical studies on sporadic ALS, superoxide dismutase 1 (SOD1)-mutated familial ALS, and SOD1-mutated ALS animal models

Received: 21 September 2004 / Revised: 9 March 2005 / Accepted: 9 March 2005 / Published online: 28 June 2005

Abstract Peroxiredoxin-II (PrxII) and glutathione peroxidase-I (GPxI) are regulators of the redox system that is one of the most crucial supporting systems in neurons. This system is an antioxidant enzyme defense system and is synchronously linked to other important cell supporting systems. To clarify the common self-survival mechanism of the residual motor neurons affected by amyotrophic lateral sclerosis (ALS), we examined motor neurons from 40 patients with sporadic ALS (SALS) and 5 patients with superoxide dismutase 1 (SOD1)-mutated familial ALS (FALS) from two different families (frameshift 126 mutation and A4 V) as well as four different strains of the SOD1-mutated ALS models (H46R/G93A rats and G1H/G1L-G93A mice). We investigated the immunohistochemical expression of PrxII/GPxI in motor neurons from the viewpoint of the redox system. In normal subjects, PrxII/GPxI immunoreactivity in the anterior horns of the normal spinal cords of humans, rats and mice was primarily identified in the neurons: cytoplasmic staining was observed in almost all of the motor neurons. Histologically, the number of spinal motor neurons in ALS decreased with disease progression. Immunohistochemically, the number of neurons negative for PrxII/GPxI increased with ALS disease progression. Some residual motor neurons coexpressing PrxII/GPxI were, however, observed throughout the clinical courses in some cases of SALS patients, SOD1-mutated FALS patients, and ALS animal models. In particular, motor neurons overexpressing PrxII/GPxI, i.e., neurons showing redox system up-regulation, were commonly evident during the clinical courses in ALS. For patients with SALS, motor neurons overexpressing PrxII/GPxI were present mainly within approximately 3 years after disease onset, and these overexpressing neurons thereafter decreased in number dramatically as the disease progressed. For SOD1-mutated FALS patients, like in SALS patients, certain residual motor neurons without inclusions also overexpressed PrxII/GPxI in the short-term-surviving FALS patients. In the ALS animal models, as in the human diseases, certain residual motor neurons showed overexpression of PrxII/GPxI during their clinical courses. At the terminal stage of ALS, however, a disruption of this common PrxII/GPxI-overexpression mechanism in neurons was observed. These findings lead us to the conclusion that the residual ALS neurons showing redox system up-regulation would be less susceptible to ALS stress and protect themselves from ALS neuronal death, whereas the breakdown of this redox system at the advanced disease stage accelerates neuronal degeneration and/or the process of neuronal death.

S. Kato (✉) · E. Ohama
Department of Neuropathology, Institute of Neurological Sciences, Faculty of Medicine, Tottori University, Nishi-cho 36-1, 683-8504 Yonago, Japan
E-mail: kato@grape.med.tottori-u.ac.jp
Tel.: +81-859-348034
Fax: +81-859-348289

M. Kato
Division of Pathology, Tottori University Hospital, Yonago, Japan

Y. Abe · T. Matsumura · T. Nishino
Department of Biochemistry and Molecular Biology, Nippon Medical School, Tokyo, Japan

M. Aoki · Y. Itoyama
Department of Neuroscience, Division of Neurology, Tohoku University Graduate School of Medicine, Sendai, Japan

K. Asayama
Department of Pediatrics, University of Occupational and Environmental Health, Kitakyushu, Japan

A. Awaya
Japan Science and Technology Agency, Tachikawa, Japan

A. Hirano
Division of Neuropathology, Department of Pathology, Montefiore Medical Center, Bronx, New York, USA

Keywords Amyotrophic lateral sclerosis · Peroxiredoxin-II · Glutathione peroxidase-1 · Redox system

Introduction

Amyotrophic lateral sclerosis (ALS), first described by Charcot and Joffroy in 1869 [11], is a fatal and age-associated neurodegenerative disorder that primarily involves both the upper and lower motor neurons [23]. This disease has been recognized as a distinct clinicopathological entity of unknown etiology for over 130 years.

During physiological processes and in response to external stimuli such as ultraviolet radiation, cells produce reactive oxygen species (ROSs). To protect itself from these potentially destructive ROSs, each cell of the living organs has developed a sophisticated antioxidant system. In such systems, there are two groups of the enzymes: those constituting the first group convert superoxide radicals into hydrogen peroxide (H_2O_2), and those of the second convert H_2O_2 into harmless water and oxygen. The neuronal cytoplasmic isoform of the first enzyme group is superoxide dismutase 1 (SOD1) [13]. In the second enzyme group, there are the peroxiredoxin (Prx) and glutathione peroxidase (GPx) families, as well as catalase localized within peroxisomes. Unlike in SOD1 and catalase, enzymes of the Prx and GPx families require secondary enzymes and cofactors to function at high efficiency [7]. The enzymes of the Prx and GPx families are considered to play important roles in the direct control of the redox system. In general, the redox system regulates versatile control mechanisms in signal transduction and gene expression [35]. In mammalian cells, this redox signal transduction is synchronously linked to important systems such as cellular differentiation, immune response, growth control, apoptosis, and tumor growth [4, 9, 19, 26, 31, 34]. In the mammalian central nervous system (CNS), the members of Prx and GPx families regulating the neuronal cytoplasmic redox system are PrxII and GPxI, which directly control the redox system in neurons [6, 7, 8, 12, 17, 24, 27, 29, 30]. In the in vivo milieu where mutant SOD1 exists, PrxII/GPxI co-aggregates with SOD1 as neuronal Lewy body-like hyaline inclusions (LBHIs): neuronal LBHIs immunohistochemically positive for three proteins of SOD1, PrxII and GPxI are observed in the mutant SOD1-related familial ALS (FALS) patients and transgenic rats expressing human SOD1 with H46R and G93A mutations [24]. Although some motor neurons with SOD1 gene mutation form inclusions that are positive for these three proteins, other SOD1-mutated motor neurons progress to cell death without forming the inclusions.

On the other hand, an essential histopathological feature of ALS is loss of the large anterior horn cells throughout the spinal cord, with the surviving motor neurons of the spinal cord exhibiting shrinkage. Among these residual large anterior horn cells, some appear to be normal. These surviving motor neurons in ALS patients are thought to possess some form of self-preservation mechanism. To gain new insight into the survival mechanism of these residual motor neurons, we focused on the redox system. In the study presented here, we performed immunohistochemical analyses of the spinal cord, not only from FALS patients with SOD1 gene mutations and SOD1-mutated ALS animal models, but also from patients with sporadic ALS (SALS), and analyzed the expression of PrxII/GPxI (redox system) in the residual motor neurons.

Materials and methods

Autopsy specimens

Histochemical and immunohistochemical studies were performed on archival, buffered 10% formalin-fixed, paraffin-embedded spinal cord tissues obtained at autopsy from 40 SALS patients and 5 FALS patients, who were members of two different families. The main clinical characteristics of the SALS patients are summarized in Fig. 2. The clinicopathological characteristics of the FALS patients are summarized in Table 1 and have been reported previously [20, 21, 25, 28, 33, 36, 38]. SOD1 analysis revealed that the members of the Japanese Oki family had a two-base pair deletion at codon 126 (frameshift 126 mutation) [20] and that the members of the American C family had an Ala to Val substitution at codon 4 (A4V) [36]. As controls for human samples, we examined autopsy specimens of the spinal cord from 20 neurologically and neuropatho-

Table 1 Characteristics of five FALS cases (*FALS* familial amyotrophic lateral sclerosis, *SOD* superoxide dismutase, *LBHI* Lewy body-like hyaline inclusion, *2-bp* two-base pair, *PCI* posterior column involvement type, + detected, *ND* not determined, *As* asphyxia, *IH* intraperitoneal hemorrhage, *RD* respiratory distress, *Pn* pneumonia)

Case	Age	Sex	Cause of death	FALS duration	SOD1 mutation	FALS subtype	Neuronal LBHI
Japanese Oki family							
1	46	F	As	18 months	2-bp deletion (126)	PCI	+
2	65	M	IH	11 years	2-bp deletion (126)	PCI and degeneration of other systems	+
American C family							
3	39	M	RD	7 months	A4V	PCI	+
4	46	M	Pn	8 months	A4V	PCI	+
5	66	M	Pn	1 year	ND	PCI	+

logically normal individuals (11 males, 9 females; aged 37–75 years).

Animal models

Histochemical and immunohistochemical studies were also carried out on specimens from ALS animal models: transgenic rats and mice carrying the overexpressed human mutant SOD1 genes. The H46R rats used in this study were a transgenic line (H46R-4) in which the level of human SOD1 with the H46R mutation was 6 times the level of endogenous rat SOD1 [32]. The G93A rats were a transgenic line (G93A-39) in which the level of human SOD1 with the G93A mutation was 2.5 times the level of endogenous rat SOD1 [32]. The G93A mice used in this study represented two lines of transgenic mice carrying the overexpressed human G93A mutant SOD1 gene: high copy G93A mice [B6SJL-TgN(SOD1-G93A)1Gur, JR2726; G1H-G93A] and low copy G93A mice [B6SJL-TgN(SOD1-G93A)1Gur^{dl}, JR2300; G1L-G93A] (Jackson Laboratory, Bar Harbor, ME). The H46R rats were killed at 110 ($n=1$), 135 ($n=1$), 160 ($n=1$), 170 ($n=1$), and over 180 ($n=3$) days after birth. The G93A rats were killed at 70 ($n=1$), 90 ($n=1$), 110 ($n=1$), 130 ($n=1$), 150 ($n=1$), and over 180 ($n=3$) days after birth. The detailed clinical signs and pathological characteristics of the H46R and G93A rats have been demonstrated previously [32]. As rat controls, we investigated the spinal cord specimens of each of eight age-matched littermates of the H46R and G93A rats. The G1H-G93A mice were examined at 90 ($n=2$), 100 ($n=2$), 110 ($n=3$), and 120 ($n=3$) days of age. The G1L-G93A mice were examined at 90 ($n=1$), 100 ($n=1$), 120 ($n=1$), 150 ($n=1$), 180 ($n=1$), 190 ($n=1$), 215 ($n=1$), 230 ($n=1$), and over 250 ($n=2$) days of age. As mouse controls, we also examined the spinal cord specimens of each of ten age-matched littermates of the G1H-G93A and G1L-G93A mice. Rats and mice were anesthetized with sodium pentobarbital (0.1 ml/100 g body weight). After perfusion of the animals via the aorta with physiological saline at 37°C, they were fixed by perfusion with 4% paraformaldehyde in 0.1 M cacodylate buffer (pH 7.3). The spinal cords were removed and then postfixed in the same solution. This study was approved by the Institutional Animal Care and Use Committee of Tottori University (Permission no. 03-S-18).

Histochemistry and immunohistochemistry

After fixation, the specimens were embedded in paraffin, cut into 6-μm-thick sections and examined by light microscopy. Spinal cord sections were stained by the following histochemical methods: hematoxylin and eosin (HE), Klüver-Barrera, Holzer, phosphotungstic acid-hematoxylin, periodic acid-Schiff, alcian blue, Masson's trichrome, Mallory azan, and Gallyas-Braak stains.

Rat PrxII, which contained a 6-His-tagged sequence at the N-terminal region, was overexpressed using *Escherichia coli* strain BL21 (DE3) cells harboring the expression plasmid pET30a (Novagen, Darmstadt, Germany) -PrxII, according to the modified method by Hirotsu et al. [15]. The His-tagged PrxII induced with 0.1 mM isopropyl-β-D-thiogalactoside (IPTG) was purified by a Ni^{2+}-nitrilotriacetate column (Qiagen, Hilden, Germany) and then digested with enterokinase. Finally, the purified PrxII was passed through an Erapture Agarose column for removal of enterokinase (Novagen). The PrxII gene was prepared from a rat liver cDNA library (Takara Biomedicals, Otsu, Japan) by PCR using the primers, 5'-TTCCATGGCCTCCGGCAACGCGCACAT-3' and 5'-TTGGATCCATCTCAGTTGTGTTTGGAG-3'. Utilizing this purified recombinant rat Prxll protein (amino acids 1–198), we produced a rabbit polyclonal antibody against rat PrxII according to the method previously described by Kato et al. [24].

Representative paraffin sections were used for immunohistochemical assays. The following primary antibodies were used: a rabbit polyclonal antibody against rat Prxll (amino acids 1–198) [diluted 1:2,000 in 1% bovine serum albumin-containing phosphate-buffered saline (BSA-PBS), pH 7.4]; an affinity-purified rabbit antibody against a synthetic peptide corresponding to the C-terminal region of Prxll (amino acids 184–198; this amino acid sequence is homologous with those of the C-terminal regions of the human, rat or mouse Prxll.) (concentration: 1 μg/ml) [24]; a polyclonal antibody to GPxl [diluted 1:2,000 in 1% BSA-PBS, pH 7.4] [3]; a polyclonal antibody to human SOD1 (diluted 1:10,000 in 1% BSA-PBS, pH 7.4) [2]; and a monoclonal antibody to human SOD1 (concentration: 3 μg/ml; MBL, Nagoya, Japan). Sections were deparaffinized, and endogenous peroxidase activity was quenched by incubation for 30 min with 0.3% H_2O_2. The sections were then washed in PBS. Normal sera homologous with the secondary antibodies were used as a blocking reagent. Tissue sections were incubated with the primary antibodies for 18 h at 4°C. PBS-exposed sections served as controls. As a further control, some sections were incubated with the polyclonal antibody against rat Prxll that had been preabsorbed with an excess amount of the recombinant rat Prxll protein. Bound antibodies were visualized by the avidin-biotin-immunoperoxidase complex (ABC) method using the appropriate Vectastain ABC kits (Vector Laboratories, Burlingame, CA) and 3,3'-diaminobenzidine tetrahydrochloride (DAB; Dako, Glostrup, Denmark) as chromogen.

Western blot analysis

This analysis was carried out on three fresh autopsy specimens from spinal cord cervical segments obtained from two SALS cases [2.5 years after onset (case 19 in Fig. 2: age 63 years) and 11 years 5 months after onset

(case 40 in Fig. 2: age 51 years)] and one normal individual (age 68 years). In brief, specimens were homogenized in Laemmli sample buffer (Bio-Rad, Hercules, CA) containing 2% sodium dodecyl sulfate (SDS), 25% glycerol, 10% 2-mercaptoethanol, 0.01% bromophenol blue, and 62.5 mM TRIS-HCl (pH 6.8). The samples were heated at 100°C for 5 min. Soluble protein extracts (20 μg) from the samples were separated on SDS-polyacrylamide gels (4–20% gradient, Bio-Rad) and transferred by electroblotting to Immobilon PVDF (Millipore, Bedford, MA). After blocking with 5% nonfat milk for 30 min at room temperature, the blots were incubated overnight at 4°C with the antibodies against Prxll and GPxl. Binding to Prxll and GPxl was visualized with the Vectastain ABC Kit and DAB. Appropriate molecular weight markers (Bio-Rad) were included in each run.

Results

Histopathology

An important histopathological finding in the spinal cord in SALS was loss of motor neurons throughout the

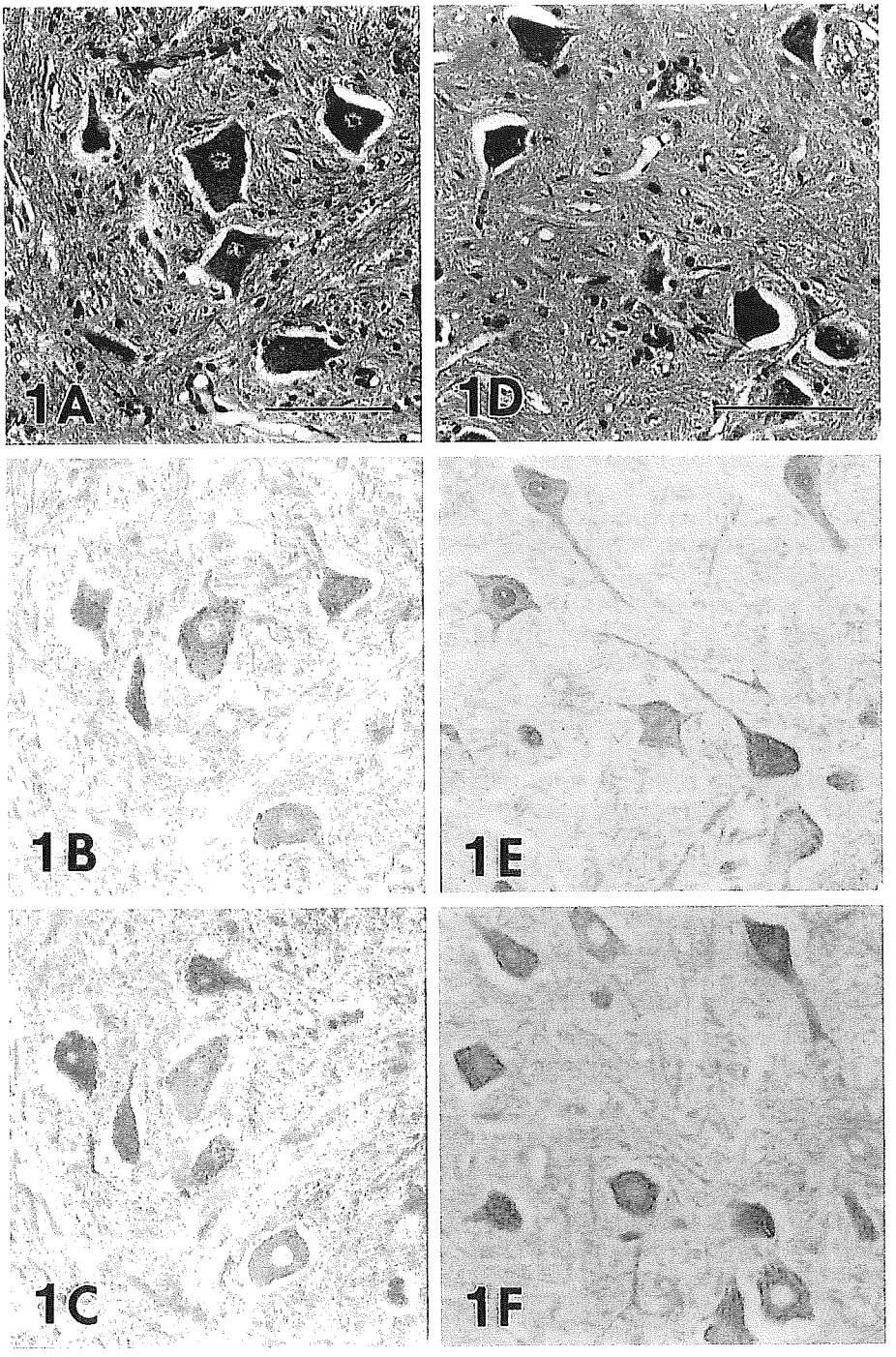

Fig. 1 Detection of PrxII and GPxI in serial sections of the normal anterior horn cells of the spinal cord in humans (**A–C**) and rats (**D–F**). **A, D** HE staining. **B, E** Immunoreactive for PrxII: immunostaining with the antibody against synthetic peptide corresponding to the C-terminal region of Prxll (**B**) and immunostaining with the antibody to rat PrxII (**E**). Immunoreactivity is identified in most of the anterior horn cells. **C, F** Immunostaining for GPxI. Almost all of the anterior horn cells in the spinal cord coexpress both PrxII (**B, E**) and GPxI (**C, F**) in comparison with HE-stained serial sections (**A, D**), although their staining intensities in neurons vary. **B, C, E, F** No counterstaining. (*HE* hematoxylin and eosin, *PrxII* peroxiredoxin-II, *GPxI* glutathione peroxidase-I). *Bars* **A** (also for **B, C**), **D** (also for **E, F**) 100 μm

course of the disease. In the specimens we examined, neuronal loss was most easily recognized in the cervical and lumbar enlargements. The surviving motor neurons showed shrinkage, and lipofuscin granule-filled neurons stood out. Among the residual motor neurons, some appeared to be normal. Bunina bodies were observed in the residual motor neurons. The number of motor neurons decreased with SALS disease progression. Reactive astrocytosis and gliosis were also observed in the affected areas. In the affected antero-lateral columns that were most pronounced in the crossed and uncrossed corticospinal tracts, there was a loss of large myelinated fibers in association with variable degrees of astrocytic gliosis. Fiber destruction was associated with the appearance of lipid-laden macrophages. Analysis of the essential changes in the five cases of SOD1-mutated FALS revealed a subtype of FALS with posterior column involvement (PCI). This subtype is characterized by degeneration of the middle root zones of the posterior column, Clarke nuclei, and the posterior spinocerebellar tracts, in addition to spinal cord motor neuron lesions. A patient who had survived for a long period, with a clinical course of 11 years (case 2 in Table 1), showed multi-system degeneration in addition to the features of FALS with PCI. Neuronal LBHIs were present in all five FALS cases with SOD1 gene mutations. The spinal cords of normal human individuals did not exhibit any distinct histopathological alterations.

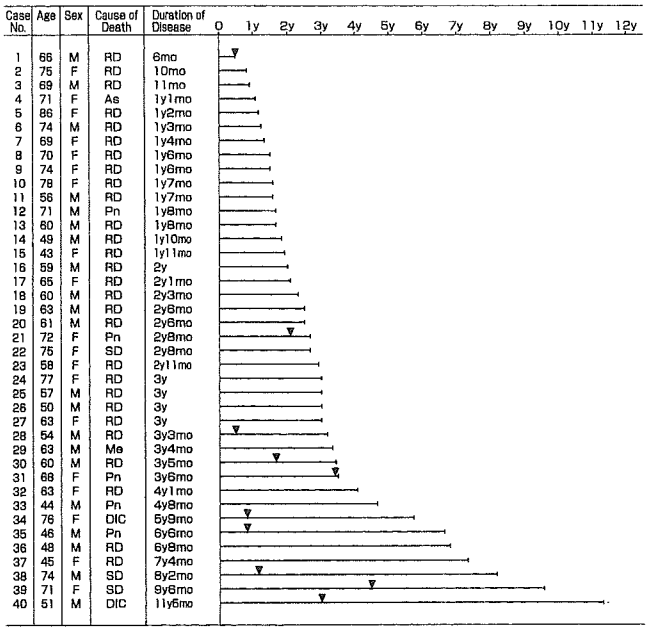

Fig. 2 Characteristics of 40 SALS cases, including patient's age, sex, cause of death, and duration of disease. The *horizontal lines* each show the duration of disease. *Arrowheads* indicate the time point at which the patients were placed on respirators (*ALS* amyotrophic lateral sclerosis, *SALS* sporadic ALS, *RD* respiratory distress, *As* asphyxia, *Pn* pneumonia, *SD* sudden death, *Me* melena, *DIC* disseminated intravascular coagulation, *y* years, *mo* months)

The clinical courses and histopathological findings of H46R and G93A transgenic rats have been reported previously by Nagai et al. [32]. As expected, the H46R rats developed motor deficits at approximately 145 days of age, and G93A rats showed the clinical signs at around 125 days of age. When we focused on the anterior horn cells, the number of the anterior horn cells of the H46R rat at 110 days of age was not significantly decreased as compared with that of the age-matched littermate. There were slightly decreased numbers of anterior horn cells with inclusions in the H46R rat at 135 days of age. At 160, 170 and over 180 days of age, the number of the anterior horn cells in the H46R rats was decreased markedly, and many inclusions including neuronal LBHIs were observed as inclusion pathology. For G93A rats, the number of the anterior horn cells at 70, 90 and 110 days of age was almost the same as that of their age-matched littermates, although at 90 and 110 days of age these rats showed vacuolation pathology including neuropil vacuoles. In G93A rats at 130, 150 and over 180 days of age, there was marked loss of the anterior horn cells, with both inclusion and vacuolation pathologies being involved. In the transgenic mice from the Jackson Laboratory, the clinical onset of the G1H-G93A mice was, as expected, about 100 days after birth, and that of G1L-G93A mice was approximately 185 days after birth. The number of the anterior horn cells of the G1H-G93A mice examined at 90 days after birth was not significantly decreased as compared with that of their age-matched littermates, whereas neuropil vacuolation was observed. The number of anterior horn cells of the G1H-G93A mice at 100 days of age was slightly decreased, and they had abundant vacuoles and a few inclusions. The G1H-G93A mice examined at 110 and 120 days of age revealed severe loss of the anterior horn cells and both inclusion and vacuolation pathologies. In the G1L-G93A mice examined at 90, 100, 120, 150 and 180 days after birth, the number of the anterior horn cells was not significantly changed compared to that of their age-matched littermates, although the G1L-G93A mice at 90, 100, 120, 150 and 180 days of age showed vacuolation pathology and, at 180 days of age, a few inclusions. In G1L-G93A mice at 190, 215, 230 and over 250 days of age, there were significant losses of anterior horn cells, with both inclusion and vacuolation pathologies being present. The spinal cords of the littermates of these animal models did not exhibit any distinct histopathological changes.

Immunohistochemistry

In the present study, we produced a rabbit polyclonal antibody against rat Prxll (amino acids 1–198), in addition to the affinity-purified rabbit antibody against a synthetic peptide corresponding to the C-terminal region of Prxll previously reported by Kato et al. [24]. This newly produced rabbit polyclonal antibody against rat Prxll was successfully applied to stain paraffin sections

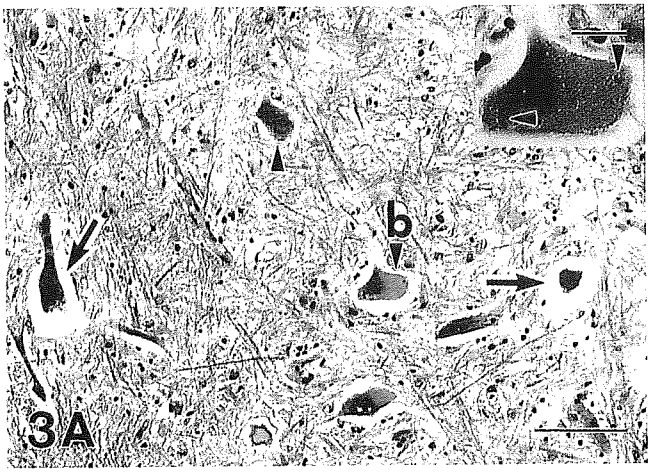

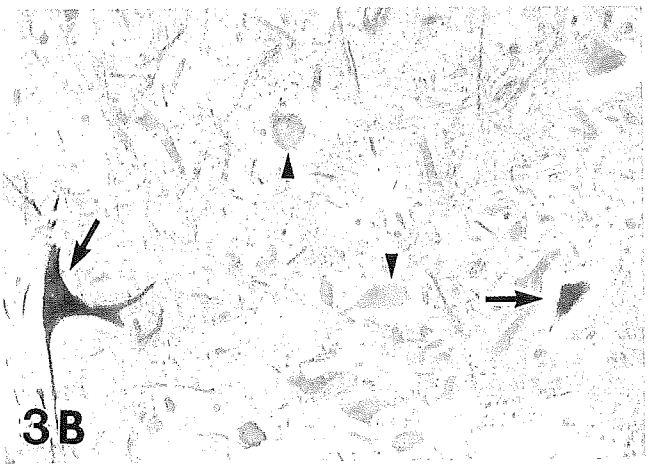

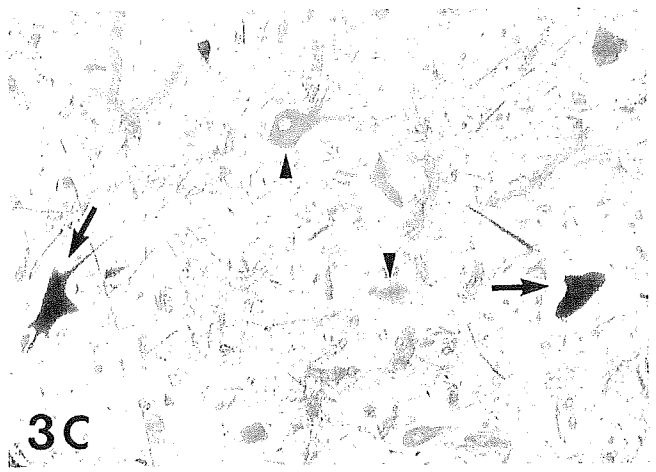

Fig. 3 Serial sections of the spinal anterior horn cells in a patient with SALS after a clinical course of 2.5 years (case 19 in Fig. 2). **A** Light microscopic preparation stained with HE. *Top right inset* shows the higher magnification of a neuron (indicated by *arrowhead* with **b** in **A**), in which Bunina bodies (*arrowheads* in *top right inset*) are observed. **B** PrxII immunoreactivity of the section consecutive to that shown in **A**. **C** GPxI immunoreactivity of the section consecutive to that shown in **B**. Residual neurons overexpressing both PrxII and GPxI are evident (*arrows*). The staining pattern is diffuse in the cytoplasm and dendrites. Other neurons are either faintly stained by both antibodies, or unstained (*arrowheads*). Observation of only the HE-stained section in **A** reveals no difference between the neurons overexpressing PrxII/GPxI and those almost negative for PrxII/GPxI. No correlation is demonstrated between PrxII/GPxI expression and the presence of Bunina bodies. **B**, **C** No counterstaining. *Bar* **A** (also for **B**, **C**) 100 μm, *top right inset* in **A** 20 μm

from rats (Fig. 1E). Additionally, we were able to use this rabbit polyclonal antibody against rat Prxll to stain paraffin sections from humans and mice. Both anti-Prxll antibodies had the same ability to immunostain paraffin sections from humans, rats and mice, as well as in immunoblotting of tissue homogenate of the human spinal cord. When control and representative paraffin sections were incubated with PBS alone (i.e., no primary antibody), no staining was detected. Incubation of sections with anti-rat Prxll antibody that had been pretreated with an excess amount of the recombinant rat Prxll protein (amino acids 1–198) produced no staining in any of the sections.

As expected [24], almost all of the normal anterior horn cells in the spinal cords of humans, rats and mice coexpressed both Prxll and GPxl (Fig. 1), although their staining intensities in positively stained neurons varied. With respect to the intracellular localization of Prxll using the two anti-Prxll antibodies, immunostaining of the neuronal cytoplasm and proximal dendrites was specifically observed (Fig. 1B, E). In addition, the nuclei of some neurons were immunostained, albeit the staining intensity varied (Fig. 1E). GPxl immunostaining showed a cytoplasmic staining pattern, with the cell bodies and proximal dendrites being essentially identified (Fig. 1C, F), but no intranuclear staining was observed (Fig. 1C, F).

In SALS patients, some residual neurons expressed both Prxll and GPxl strongly within about 3 years after disease onset (cases 1–27 in Fig. 2). Other neurons were either faintly stained by both antibodies or unstained. Around 2–3 years after disease onset in SALS patients (cases 16–27 in Fig. 2), the intensity of Prxll and GPxl immunoreactivities peaked in some residual neurons that were positive for both proteins (Fig. 3). In SALS patients with a clinical course of over 3 years (cases 28–40 in Fig. 2), the number of residual neurons decreased strikingly, and respiratory assistance became essential for most patients. The residual neurons intensely expressing both Prxll and GPxl decreased with disease progression, while the number of residual neurons negative for both proteins increased dramatically (Fig. 4). At 11 years 5 months after disease onset (case 40 in Fig. 2), most of the neurons were atrophic and immunonegative for both Prxll and GPxl. However, even in this long-surviving patient, a few residual neurons expressing both Prxll and GPxl were observed (Fig. 5). Thus, residual motor neurons positive for both Prxll and GPxl were always evident throughout the disease course in every SALS patient, although after approximately 3 years of disease their number decreased dramatically. Observation of only the HE-stained sections revealed no